Differential impact of TGFβ/SMAD signalling activity elicited by Activin A and Nodal on endoderm differentiation of epiblast stem cells

Hilary Knowles, Nicole Santucci, Joshua Studdert, Hwee Ngee Goh, Keren Kaufman-Francis, Nazmus Salehin, Patrick Tam, Pierre Osteil

REVISON DOCUMENT

Differential impact of TGFβ/SMAD signalling activity elicited by Activin A and Nodal on endoderm differentiation of epiblast stem cells

Hilary Knowles[1], Nicole Santucci[1], Joshua Studdert[1], Hwee Ngee Goh[1], Keren Kaufman-Francis[1], Nazmus Salehin[1,2], Patrick P L Tam[1,2] and Pierre Osteil[1,2,3]

[1] Embryology Research Unit, Children's Medical Research Institute, University of Sydney, Westmead, NSW Australia and [2] School of Medical Sciences, Faculty of Medicine and Health, University of Sydney, NSW Australia. [3] Swiss Cancer Research Institute (ISREC), School of Life Sciences, Ecole Polytechnique Fédérale de Lausanne (EPFL), Lausanne, Switzerland.

Acknowledgements

Flow cytometry experiments were performed at the Westmead Scientific Platforms, which are supported by the Westmead Research Hub, the Cancer Institute New South Wales, the National Health and Medical Research Council of Australia (NHMRC) and the Ian Potter Foundation. This work was supported by National Health and Medical Research Council of Australia (Grant 632776), the Australian Research Council (DP 160103651) and Mr James Fairfax. PO was supported by Sir Norman Gregg Research Fellowship and PPLT by NHMRC Research Fellowship (1110751).

Conflict of Interest Statement

The authors declare no conflicts of interest

ABSTRACT

Allocation of cells to an endodermal fate in the gastrulating embryo is driven by Nodal signalling and consequent activation of TGFβ pathway. *In vitro* methodologies striving to recapitulate the process of endoderm differentiation, however, used TGFβ family member Activin in place of Nodal. This is despite Activin not known to have an *in vivo* role in endoderm differentiation. In this study, five Epiblast Stem Cell lines were subjected to directed differentiation using both Activin A and Nodal to induce endodermal fate. A reporter line harbouring endoderm markers *FoxA2* and *Sox17* was further analysed for TGFβ pathway activation and WNT response. We demonstrated that Activin A treated cells remain more primitive streak-like when compared to Nodal treated cells that have a molecular profile suggestive of more advanced differentiation. Activin A elicited a robust TGFβ/SMAD activity, enhanced WNT signalling activity and promoted the generation of DE precursors. Nodal treatment resulted in lower TGFβ/SMAD activity, and a weaker, sustained WNT response, and ultimately failed to upregulate endoderm markers. This is despite signalling response resembling more closely the activity seen *in vivo*. These findings emphasise the importance of understanding the downstream activities of Activin A and Nodal signalling in directing *in vitro* endoderm differentiation of primed-state epiblast stem cells.

INTRODUCTION

During gastrulation, the epiblast cells are allocated to the precursors of ectoderm, mesoderm and definitive endoderm (DE) lineages. The differentiation of epiblast cells to the DE precursors is driven Transforming Growth Factor (TGF)β / Nodal signalling activity as well as WNT signalling (Gadue et al., 2006; Tam & Behringer, 1997).

Cytokines of the TGFβ superfamily are functionally divided into two subfamilies; the Nodal subfamily (which includes Activins), and the BMP subfamily (Schmierer & Hill, 2007). Ligands of both TGFβ subfamily signal through receptor complexes consisting of type I (or ALK) receptors and constitutively active type II (ActRII) receptors. Upon ligand binding, ALK receptors are phosphorylated and transduce intracellularly via phosphorylation of SMAD proteins (Massagué et al., 2005). Nodal and BMP subfamily ligands are transduced through separate downstream SMAD cascades. BMP family ligand binding results in SMAD1, SMAD5 and SMAD8 (SMAD1/5/8) phosphorylation (Chang et al., 2000; Huang et al., 2009; Massagué et al., 2005), whereas Nodal family ligands on the other hand induce phosphorylation of SMAD2 and SMAD3 (SMAD2/3) (Massagué et al., 2005; Wu et al., 2000). Nodal binding to ALK4/ActRII requires co-receptor Cripto (encoded by *Tdgf1*) (Yan et al., 2002; Yeo & Whitman, 2001). Specifically, Cripto functions as a co-receptor to Nodal when membrane bound by a glycosylphosphatidylinositol-anchor (GPI-anchor). Cleavage of Cripto from the GPI-anchor results in a shortened, biologically active soluble protein (Lee et al., 2016; Yan et al., 2002). Activin is capable of signalling without Cripto, with Activin binding to the ActRII receptor (Gray et al., 2003). Loss-of function (LOF) mutation of Nodal or Cripto results in defective gastrulation *in vivo* (Ding et al., 1998; Gu et al., 1998). In studies examining Embryonic Stem Cell (ESC) priming for cardiomyocyte differentiation, a dose-dependent increase of soluble Cripto is observable after Activin treatment (Duelen et al., Parisi et al.).

In an *in vivo* context, Nodal signalling induces expression of WNT antagonists, contributing to the patterning of the primitive streak (Perea-Gomez et al., 2002). Without Wnt3 activity, mesoderm derivatives do not emerge at the primitive streak (Liu et al., 1999), and *Wnt3*-null embryos are phenotypically similar to mesoderm-deficient development embryos (Hsieh et al., 2003). Inhibition of WNT signalling downstream regulator β-catenin is also implicated in disruption of cell allocation to the DE *in vivo* (Lickert et al., 2002). The role of WNT in endoderm allocation is seemingly dose-dependent, with *in vitro* human ESC modelling demonstrating low WNT doses are conducive for endoderm differentiation, whilst high doses induce mesodermal fate (Jiang et al., 2021).

Nodal signalling *in vivo* is essential for the generation of DE (Grapin-Botton & Constam, 2007; Schier, 2003; Stainier, 2002; Zorn & Wells, 2007). However, DE differentiation of stem cells *in vitro* has utilised another TGFβ family member, Activin A, as a substitute for Nodal in driving endoderm differentiation. This is despite embryological studies revealing that mRNA encoding all three subunits of Activin are present in the ICM of the E3.5 mouse, and then restricted to the trophectoderm and E11.5 liver, yet not in the primitive streak of the gastrulating mouse embryo (Albano et al., 1993). Knockout of both Activin beta-chains leads to complete loss of Activin function, craniofacial defects and early postnatal lethality (Kuehn et al., 2001; Lau et al., 2000), demonstrating that Activins are expressed during development but may play no role in gastrulation and endoderm formation. Furthermore, Activins seem incapable of regulating Nodal antagonist *Lefty* (C. Chen & Shen, 2004). *Lefty1*$^{-/-}$ mice fail to

regulate primitive streak marker *Brachyury*, resulting in the formation of multiple primitive streaks and failure of germ layer formation (Perea-Gomez et al., 2002).

Whilst the extensive role of Nodal signalling has been examined *in vivo*, the question of whether Activin A and Nodal act similarly to promote endoderm differentiation remains open. A previous study has shown that, in directing the differentiation of ESCs to pancreatic islet cells, induction by Activin A or Nodal produced functionally disparate endoderm precursor cells (A. E. Chen et al., 2013). While cells derived from stem cells cultured with either factor expressed the typical DE markers, FOXA2 and SOX17, and were indistinguishable on the basis of transcriptome, Activin A-derived cells, in contrast to the Nodal-derived cells, could not contribute to endoderm cells in primitive gut tube of the chimeric embryo, nor could they differentiate into pancreatic cells *in vitro* efficiently.

Another example of the disparate action of Nodal and Activin A was found during the induction of endoderm differentiation of isogenic epiblast stem cells (EpiSCs) derived from the epiblast of post-implantation mouse embryo (Kojima et al., 2014). When these EpiSCs are differentiated in serum-supplemented medium, they display different capacity to generate DE-like cells and progenitors of hepatocytes, cholangiocytes and pancreatic islet cells. EpiSCs with enhanced endoderm propensity – characterised by an early onset of *Mixl1* expression - respond to both Activin A and Nodal induction to generate endoderm derivatives efficiently, while those with poor propensity fail to respond to either factor and those with suboptimal propensity for endoderm differentiation respond to Activin A more robustly than Nodal (Kaufman-Francis et al., 2014).

In the present study, the molecular activity underpinning the differential response to Activin A and Nodal was examined during the first 4 days of induced *in vitro* differentiation of EpiSCs with suboptimal endoderm propensity. The findings demonstrate that Activin treatment promotes an endodermal outcome whilst Nodal is incapable of driving endoderm. Assessment of the underlying TGFβ pathway reveal that Nodal is unable to activate downstream TGFβ/SMAD transduction and WNT signalling in the EpiSCs in a manner required for endoderm differentiation *in vivo*. This cell line-specific response highlights the importance of optimising the use of Activin A in place of Nodal when directing endoderm differentiation of pluripotent stem cells.

RESULTS

Activin A and Nodal elicit specific SMADs transduction

In the gastrulating embryo, Nodal in the anterior primitive streak (APS) signals through the TGFβ pathway. To study the TGFβ response *in vitro*, an APS-counterpart EpiSC line (FS09), was established from the embryo of the mouse harbouring the Foxa2-Venus and Sox17-mCherry reporter (Burtscher et al., 2013). To elucidate whether differences in response are related to activation of the TGFβ signalling pathway, FS09 cells were treated with three factors of the TGFβ superfamily; Activin A, Nodal and BMP4. EpiSC cells require low levels of Activin A (20ng/mL) supplementation to maintain pluripotency, with TGFβ pathway inhibition (by small molecule SB431542) resulting in loss of pluripotency markers (Chenoweth & Tesar, 2010; Vallier et al., 2009). Therefore, to observe the impact of TGFβ treatment in driving cells away from the maintained pluripotent state, factors were added at three concentrations above the maintenance condition (50, 100 and 200 ng/mL). Treated cells were collected after 48 hours of *in vitro* 2D culture, alongside untreated cells in control conditions (culture medium without factors), to evaluate the status of the signalling pathway after long term treatment.

To examine TGFβ pathway response to Activin A, Nodal and BMP4, we probed for the phosphorylated forms of the downstream activators of both subfamilies. pSMAD2/3 levels increased with the concentration of Activin A, whereas Nodal induction peaked at 50-100 ng/mL and decreased with higher concentration, to a level comparable to that of BMP4 treated and untreated cells (Figure 1A and B, Figure S1A and B). Untreated and BMP4 treated EpiSCs maintained a high level of pSMAD1/5/8 while both Nodal and Activin A lowered the pSMAD1/5/8 level, with Activin A displaying the strongest effect (Figure 1A and B).

Faial et al. (2015) demonstrated that SMAD2/3 induced expression of *Eomes* resulted in decreased *Brachyury* expression, and SMAD1/5/8 induction produced the inverse result. Accordingly, in qPCR analysis of samples shown in Fig. 1A , *Eomes* expression (relative to control EpiSCs collected 48hrs post seeding) was significantly upregulated by 200ng/mL Activin-A treatment when compared to the corresponding BMP4 treatment (Figure 1C). Conversely, *Brachyury* expression was significantly increased with BMP4 treatment at 200ng/mL when compared to Activin treatment (Figure 1D). Nodal treatment failed to follow the trend; comparing Activin A and BMP4 treatments, *Eomes* response was significantly lower at 100ng/mL and 200ng/mL than corresponding Activin A treatments. However, Nodal treatment did not inversely drive *Brachyury* expression, with Nodal treatment resulting in lower expression than BMP4 treatment at 100ng/mL and 200ng/mL (Figure 1C and D).

qPCR analysis demonstrated that supplementation of media with Nodal or Activin A promoted increased expression of endodermal marker *Sox17* above the control baseline (of cells cultured in factor-free EpiSC medium), while BMP4 treated cells did not show *Sox17* upregulation (Figure 1E). The strongest induction was achieved with Activin A at 200ng/mL (Figure 1E).

As both SMAD2/3 and SMAD1/5/8 are regulated by shared TGFβ pathway components (e.g., SMAD4), pathway activation is suggested to be competitive. Treatment of FS09 EpiSCs with Activin A, Nodal and BMP4 revealed a trend of negative correlation between pSMAD2/3 and pSMAD1/5/8 western blot band strength ($r = -0.622$, $p = 0.0034$; Pearson correlation), with BMP4 treatment being the more active in driving phosphorylation of pSMAD1/5/8, and Activin A driving phosphorylation of pSMAD2/3 (Figure 1F). These findings demonstrate Activin A is more potent at activating pSMAD2/3 than Nodal, while both appear involved in dampening the activation of pSMAD1/5/8.

EpiSCs follow different cell trajectories under Nodal and Activin A induction

To evaluate the ability Activin and Nodal to drive cells from a pluripotent state into lineage specification, five EpiSC lines were differentiated towards DE using a directed embryoid body (EBs) protocol (see methods). Samples were collected at Day 2 and Day 4 of differentiation, as well as at Day 0, immediately prior to factor addition (control), and assessed for gene expression using high-throughput qPCR (Biomark – see Methods).

Cell lines CAV2, LMS3, PS03, PS04 (see Kojima et al. 2014) and FS09 (this study) were assessed via Principal Component Analysis (PCA). Two independent analyses were performed with a different set of primers targeting genes of early embryonic development (Supplementary Table 1). This screen revealed EpiSC lines followed divergent lineage trajectories over a 4-day period of *in vitro* differentiation. Globally, Nodal treatment induced a larger transcriptomic difference than Activin A, accounting for a higher Principal Component (PC) variance, when compared to control cells (Figure 2A and S2A). This result is in accordance with previous findings (Kaufman-Francis et al. 2014) where Activin and Nodal drove differentiation of the above cell lines along different trajectories. After 4 days of differentiation, Activin A induced cells displayed higher expression of pluripotency markers (*Pou5f1*,

Nanog and *Fgf5*), primitive streak markers (*Mixl1* and *T*) and early epithelial to mesenchymal transition (EMT) markers (*Cdh1*, *Twist1*). On the other hand, Nodal treatment upregulated genes associated with advanced EMT (*Cdh2*, *Vim*) (Figure 2B, 2C, 2D and S2B). In addition, Nodal was responsible for triggering a higher expression of SMAD genes toward the end of differentiation when compared to Activin. Activin treated cells display a profile that is closer to the control cells at Day 0 and to a primitive streak stage, as suggested by the maintained expression of *Mixl1* and *T* (Figure 2C and D). Despite Nodal inducing a gene expression profile suggestive of more advanced differentiation, endoderm marker *Sox17* expression was not consistent across analysis, indicating a sub-optimal endoderm differentiation protocol using Nodal (Figure 2C and D).

Overall, our analysis demonstrated that Nodal induced EpiSC differentiation resulted in a gene expression profile divergent to that of Activin treatment. Analysis suggests Activin treated cells may remain more primitive streak-like when compared to Nodal treated cells that displayed a molecular profile suggestive of more advanced differentiation.

Signalling activities elicited by Activin A and Nodal diverge during endoderm differentiation

To assess the ability of factors to effectively induce DE differentiation, the presence of Foxa2-Venus::Sox17-mCherry positive cells in FS09-derived EBs was assessed. EBs were cultured in factor-free serum replacement medium with supplementation of Activin A or Nodal and assessed by fluorescence microscopy (Figure 3A) and FACS analysis (Figure 3B) over 4 days of differentiation. Activin A treated EBs displayed peak preponderance of Foxa2+ and dual Foxa2+/Sox17+ cells at day 2, with 25% of the cells in EBs being Foxa2+, and about 3% both Foxa2+ and Sox17+ (Figure 3C). A small yet detectable fraction of Sox17+ cells were present with Activin A treatment at days 1-3 (Figure 3B). In contrast to the outcome of 2D culture, Nodal-treated EBs did not produce Foxa2+, Sox17+ or dual Foxa2+/Sox17+ cells. In the control EB condition (culture medium without factors), less than 5% of cells expressed FoxA2–Venus by day 4 of differentiation, suggesting that control condition was sufficient for minimal undirected differentiation towards the endoderm.

To examine the role of TGFβ signalling in driving unique differentiation outcomes after Activin or Nodal treatment (both at 100ng/mL), the expression of pSMAD2 and pSMAD1/5/8 was assessed. Samples of FS09 cells were collected over four days of EB differentiation for western blot analysis (Figure 4A, Figure S1B). Quantification of the band intensity relative to vinculin control (n=2) showed that Activin A upregulated pSMAD2 expression, reaching an elevated plateau level by Day 2(Figure 4B). Nodal has little effect on pSMAD2 expression, and the level did not differ from Day 0 expression or from the control (Figure 4B). Both Activin A and Nodal downregulated pSMAD1/5/8 activity from Day 1 of differentiation and the activity remained low over days 2-4 (Figure 4B). pSMAD1/5/8 remained expressed in untreated cells during differentiation, indicating endogenous BMP signalling was active in the FS09 EpiSCs. That Nodal and Activin A treatments shut down pSMAD1/5/8 suggested that the primary action of these factors may be to counteract BMP activity. Together, the results indicate Activin A enhanced pSMAD2 function more effectively than Nodal, however both factors are active in repressing BMP-pSMAD1/5/8 signalling activity.

We next examined if response to Nodal signalling during differentiation was modulated by Cripto, a co-receptor required for Nodal binding to ALK4/ActRII receptors (Yan et al., 2002; Yeo & Whitman, 2001). We analysed Cripto expression during differentiation with Activin A or Nodal via western blot, with an antibody specific to both the glycosylated (membrane bound, 36kDa) and unmodified (soluble, 18kDa) protein (Figure 4C, Figure S1C). Activin-A treated EpiSCs expressed membrane-anchored Cripto

on Day 1-3 of differentiation, with levels progressively decreasing to an undetectable level. However, Activin A treatment increased levels of soluble Cripto across the timeline. Membrane bound Cripto was present at a low but steady level in Nodal treated EpiSCs across this timeline, maintaining presence across all days unlike the control or Activin treated conditions. Nodal treatment did not result in detection of soluble Cripto. As Cripto is upregulated in a positive feedback loop that is initiated by Nodal and transduced by SMAD2 phosphorylation, the weak activation of SMAD2 in the Nodal-treated cells may account for the lack of Cripto upregulation in the time course of differentiation.

Nodal and Activin directed differentiation uniquely induce WNT signalling

Analysis of TGFβ pathway activity and transcriptome of differentiating EpiSCs revealed that Nodal did not induce endoderm differentiation *in vitro* as would be expected during differentiation *in vivo*. As WNT signalling activity is a requisite element of the molecular cascade driving endoderm differentiation, we next examined the activity of the WNT/β-catenin pathway by tracking the phosphorylated/active β-catenin in the differentiating EpiSCs. Treatment with Activin A was accompanied by the upregulation of active β-catenin at day 2-3. Nodal treatment, in contrast, enhanced expression of active β-catenin at later time points, day 3-4 (Figure 5A, Figure S1D). The untreated cells displayed enhanced β-catenin separately on day 1 and 3. Expression of genes associated with the canonical WNT signalling pathway were assessed. Expression of the signalling agonists, *Wnt3 and Wnt3a* was elevated following Activin A and Nodal treatment. However, while the expression of both Wnt3 and Wnt3a was maintained in the Nodal treated culture, Wnt3a expression declined in the Activin treated culture after the Day 1 peak (Figure 5B). Furthermore, the expression of signalling antagonists, *Cerberus-1 (Cer1), Goosecoid (Gsc)* and *Dickkopf 1 (Dkk1),* were enhanced by Activin A, but not by Nodal (Figure 5B). These results may suggest that Activin A has elicited antagonistic activity to modulate the level of WNT signalling activity, whereas Nodal did not elicit the antagonistic activity to effectively regulate the pathway activity across the 4-day timeline of endoderm differentiation.

Discussion

We set out to decrypt the differences in the response to signalling activity elicited by two TGFβ growth factors, Nodal and Activin A. Previous work that has comparatively explored these two ligands revealed differences in response, yet there are gaps in knowledge that this study has further explored. A. E. Chen et al. (2013), in aiming to explore the functional capacity of late endoderm derived from Activin or Nodal treatment, did not focus on the DE derived after 7 days *in vitro*. Rather, to achieve their DE population, differing concentrations of Activin A and Nodal (100ng/mL and 1000ng/mL respectively) were used, and the mixed population was sorted for DE cells prior to functional evaluation. To assess the ability of Activin A and Nodal to induce endoderm differentiation, we examined the transition from pluripotent culture, comparing Activin A and Nodal at matched concentrations. Analysis of 5 EpiSC lines revealed directed differentiation outcomes were divergent between Activin and Nodal treated cells. Activin A treatment results in a transcriptomic profile suggestive of a primitive streak outcome, with maintained *Mixl1* and *Brachyury* expression. On the other hand, genes associated with advanced EMT were upregulated after four days of Nodal treatment. Together, these results suggest improved ability for Nodal to prime for or induce differentiation.

We utilised the FS09 EpiSC line that harbours the reporter for Foxa2 and Sox17 expression, an entry point to explore the mechanisms underpinning the different outcomes of TGFβ signalling after demonstrating that they behave similarly to previously published cells (Kojima et al. 2014). Nodal does

not induce the differentiation of Foxa2+ and Sox17+ cells, while Activin A drives the differentiation of 25% of cells to Foxa2-expressing cells. We demonstrated that Activin A triggered phosphorylation of SMAD2 but low level of phosphorylation of SMAD1, while Nodal seems to achieve an intermediate level of phosphorylation for both. Nodal-mediated phosphorylation of SMAD1/2 is intermediate between Activin A and BMP4. Nodal treatment responded in steady but weak expression of membrane-anchored, co-receptor Cripto across the differentiation timeline. An inability for Nodal to upregulate Cripto expression in an *in vitro* context may partially account for failure to induce endoderm differentiation. Activin A induced differentiation was not impeded by decreasing levels of Cripto across the timeline. Activin treatment alone did induce expression of soluble Cripto, a factor reported to be crucial to avoid neural fate in Activin induced differentiation in ESCs (Parisi, 2003).

Canonical WNT signalling proteins (e.g., Wnt1, Wnt3, Wnt3a, Wnt8) lead to cellular response through stabilisation of transduction protein β-catenin, via inhibition of the β-catenin-destruction protein complex (Koyanagi et al., 2005; Zeng et al., 1997). The active form of β-catenin translocates to the nucleus and has direct gene regulatory effects (Molenaar et al., 1996). In the context of WNT signalling, active β-Catenin expression peaked at Day 2 of differentiation following Activin treatment while Nodal produced a slowly increasing but sustained activation. Treatment with both factors was accompanied by enhanced expression of *Wnt3* and *Wnt3a*, but pathway inhibitors *Cer1*, *Dkk1* and *Gsc* were activated only with Activin A treatment. WNT signalling antagonists can either directly inhibit WNT proteins from interacting with their receptors (e.g. *Cer1*), interact and maintain the β-catenin-destruction protein complex (e.g. *Dkk1*), or act as a transcriptional repressor of *Wnt* genes (e.g. *Gsc*) (Katoh & Katoh, 2006; Niida et al., 2004; Osteil et al., 2015). An endodermal, rather than mesodermal, outcome *in vivo* is closely tied to WNT pathway regulation (Perea-Gomez et al., 2002), and *in vitro* methodologies fail to induce endoderm rather than mesoderm when increased WNT signalling is present (Jiang et al., 2021). Whilst our results indicate that Nodal treatment may mimic more closely the *in vivo* condition in progressively raising WNT activity, a failure to induce WNT pathway modulators within the 4-day differentiation timeline may factor into the inability to induce DE markers *FoxA2* and *Sox17* in the FS09 cell line. This information in combination with results showing weak activation of the SMAD2/3 pathway, and equally weak inactivation of the competing SMAD1/5/8 pathway, suggest Nodal in an *in vitro* context may be unable to provide signalling cues sufficient for generating DE in differentiation methodologies commonly utilised by researchers. On the other hand, Activin A seemingly delivers unphysiologically strong signalling cues that direct the cells towards the desired fate. Data from A. E. Chen et. al (2013) and Kaufman et. al (2014), demonstrate that DE derived from Nodal treatment, rather than Activin treatment, produces more functionally competent DE derivatives. In this light, it is important to consider that the strong signalling cues seen in our results after Activin treatment may not be conducive to further endodermal applications.

Our study highlighted the importance of understanding the downstream activities of Activin A and Nodal signalling in directing endoderm differentiation of primed-state epiblast stem cells. While Nodal is not regularly used for endoderm differentiation of pluripotent stem cells, it may be the more effective factor to direct endoderm differentiation in cells of different endoderm propensity for modelling lineage differentiation and therapeutic application.

References

Albano, R. M., Groome, N., & Smith, J. C. (1993). Activins are expressed in preimplantation mouse embryos and in ES and EC cells and are regulated on their differentiation. *Development*, *117*(2), 711–723.

Burtscher, I., Barkey, W., & Lickert, H. (2013). Foxa2-venus fusion reporter mouse line allows live-cell analysis of endoderm-derived organ formation. *Genesis*, *51*(8), 596–604. https://doi.org/10.1002/dvg.22404

Chang, H., Zwijsen, A., Vogel, H., Huylebroeck, D., & Matzuk, M. M. (2000). Smad5 Is Essential for Left–Right Asymmetry in Mice. *Developmental Biology*, *219*(1), 71–78. https://doi.org/10.1006/DBIO.1999.9594

Chen, A. E., Borowiak, M., Sherwood, R. I., Kweudjeu, A., & Melton, D. A. (2013). Functional evaluation of ES cell-derived endodermal populations reveals differences between Nodal and Activin A-guided differentiation. *Development*, *140*(3), 675–686.

Chen, C., & Shen, M. M. (2004). Two modes by which Lefty proteins inhibit nodal signaling. *Current Biology*, *14*(7), 618–624.

Chenoweth, J. G., & Tesar, P. J. (2010). Isolation and maintenance of mouse epiblast stem cells. In *Cellular Programming and Reprogramming* (pp. 25–44). Springer.

Ding, J., Yang, L., Yan, Y.-T., Chen, A., Desai, N., Wynshaw-Boris, A., & Shen, M. M. (1998). Cripto is required for correct orientation of the anterior–posterior axis in the mouse embryo. *Nature*, *395*(6703), 702–707.

Faial, T., Bernardo, A. S., Mendjan, S., Diamanti, E., Ortmann, D., Gentsch, G. E., Mascetti, V. L., Trotter, M. W. B., Smith, J. C., & Pedersen, R. A. (2015). Brachyury and SMAD signalling collaboratively orchestrate distinct mesoderm and endoderm gene regulatory networks in differentiating human embryonic stem cells. *Development*, *142*(12), 2121–2135.

Gadue, P., Huber, T. L., Paddison, P. J., & Keller, G. M. (2006). Wnt and TGF-beta signaling are required for the induction of an in vitro model of primitive streak formation using embryonic stem cells. *Proceedings of the National Academy of Sciences of the United States of America*, *103*(45), 16806–16811. https://doi.org/10.1073/pnas.0603916103

Grapin-Botton, A., & Constam, D. (2007). Evolution of the mechanisms and molecular control of endoderm formation. *Mechanisms of Development*, *124*(4), 253–278.

Gray, P. C., Harrison, C. A., & Vale, W. (2003). Cripto forms a complex with activin and type II activin receptors and can block activin signaling. *Proceedings of the National Academy of Sciences of the United States of America*, *100*(9), 5193–5198. https://doi.org/10.1073/pnas.0531290100

Gu, Z., Nomura, M., Simpson, B. B., Lei, H., Feijen, A., Van Den Eijnden-Van Raaij, J., Donahoe, P. K., & Li, E. (1998). The type I activin receptor ActRIB is required for egg cylinder organization and gastrulation in the mouse. *Genes & Development*, *12*(6), 844–857.

Hsieh, J.-C., Lee, L., Zhang, L., Wefer, S., Brown, K., DeRossi, C., Wines, M. E., Rosenquist, T., & Holdener, B. C. (2003). Mesd encodes an LRP5/6 chaperone essential for specification of mouse embryonic polarity. *Cell*, *112*(3), 355–367.

Huang, Z., Wang, D., Ihida-Stansbury, K., Jones, P. L., & Martin, J. F. (2009). Defective pulmonary vascular remodeling in Smad8 mutant mice. *Human Molecular Genetics*, *18*(15), 2791–2801.

Jiang, Y., Chen, C., Randolph, L. N., Ye, S., Zhang, X., Bao, X., & Lian, X. L. (2021). Generation of

pancreatic progenitors from human pluripotent stem cells by small molecules. *Stem Cell Reports*, *16*(9), 2395–2409. https://doi.org/10.1016/j.stemcr.2021.07.021

Katoh, M., & Katoh, M. (2006). CER1 is a common target of WNT and NODAL signaling pathways in human embryonic stem cells. *International Journal of Molecular Medicine*, *17*(5), 795–799.

Kaufman-Francis, K., Goh, H. N., Kojima, Y., Studdert, J. B., Jones, V., Power, M. D., Wilkie, E., Teber, E., Loebel, D. A. F., & Tam, P. P. L. (2014). Differential response of epiblast stem cells to Nodal and Activin signalling: a paradigm of early endoderm development in the embryo. *Philosophical Transactions of the Royal Society B: Biological Sciences*, *369*(1657), 20130550.

Kojima, Y., Kaufman-Francis, K., Studdert, J. B., Steiner, K. A., Power, M. D., Loebel, D. A. F., Jones, V., Hor, A., de Alencastro, G., & Logan, G. J. (2014). The transcriptional and functional properties of mouse epiblast stem cells resemble the anterior primitive streak. *Cell Stem Cell*, *14*(1), 107–120.

Koyanagi, M., Haendeler, J., Badorff, C., Brandes, R. P., Hoffmann, J., Pandur, P., Zeiher, A. M., Kühl, M., & Dimmeler, S. (2005). Non-canonical Wnt signaling enhances differentiation of human circulating progenitor cells to cardiomyogenic cells. *Journal of Biological Chemistry*, *280*(17), 16838–16842.

Kuehn, M. R., Kumar, A., Novoselov, V., Celeste, A. J., Wolfman, N. M., & ten Dijke, P. (2001). Nodal signaling uses activin and transforming growth factor-β receptor-regulated Smads. *Journal of Biological Chemistry*, *276*(1), 656–661.

Lau, A. L., Kumar, T. R., Nishimori, K., Bonadio, J., & Matzuk, M. M. (2000). Activin βC and βE genes are not essential for mouse liver growth, differentiation, and regeneration. *Molecular and Cellular Biology*, *20*(16), 6127–6137.

Lee, G.-H., Fujita, M., Takaoka, K., Murakami, Y., Fujihara, Y., Kanzawa, N., Murakami, K.-I., Kajikawa, E., Takada, Y., Saito, K., Ikawa, M., Hamada, H., Maeda, Y., & Kinoshita, T. (2016). A GPI processing phospholipase A2, PGAP6, modulates Nodal signaling in embryos by shedding CRIPTO. *The Journal of Cell Biology*, *215*(5), 705–718. https://doi.org/10.1083/jcb.201605121

Lickert, H., Kutsch, S., Kanzler, B., Tamai, Y., Taketo, M. M., & Kemler, R. (2002). Formation of Multiple Hearts in Mice following Deletion of β-catenin in the Embryonic Endoderm. *Developmental Cell*, *3*(2), 171–181. https://doi.org/https://doi.org/10.1016/S1534-5807(02)00206-X

Liu, P., Wakamiya, M., Shea, M. J., Albrecht, U., Behringer, R. R., & Bradley, A. (1999). Requirement for Wnt3 in vertebrate axis formation. *Nature Genetics*, *22*(4), 361–365.

Massagué, J., Seoane, J., & Wotton, D. (2005). Smad transcription factors. *Genes & Development*, *19*(23), 2783–2810.

Molenaar, M., Van De Wetering, M., Oosterwegel, M., Peterson-Maduro, J., Godsave, S., Korinek, V., Roose, J., Destrée, O., & Clevers, H. (1996). XTcf-3 transcription factor mediates β-catenin-induced axis formation in Xenopus embryos. *Cell*, *86*(3), 391–399.

Niida, A., Hiroko, T., Kasai, M., Furukawa, Y., Nakamura, Y., Suzuki, Y., Sugano, S., & Akiyama, T. (2004). DKK1, a negative regulator of Wnt signaling, is a target of the β-catenin/TCF pathway. *Oncogene*, *23*(52), 8520–8526.

Osteil, P., Studdert, J., Wilkie, E., Fossat, N., & Tam, P. P. L. (2015). Generation of genome-edited mouse epiblast stem cells via a detour through ES cell-chimeras. *Differentiation*, *91*(4–5), 119–125. https://doi.org/10.1016/j.diff.2015.10.004

Parisi, S. (2003). D'Andrea D, Lago CT, Adamson ED, Persico MG, and Minchiotti G. *Nodal-Dependent Cripto Signaling Promotes Cardiomyogenesis and Redirects the Neural Fate of Embryonic Stem Cells. J Cell Biol*, *163*, 303–314.

Perea-Gomez, A., Vella, F. D. J., Shawlot, W., Oulad-Abdelghani, M., Chazaud, C., Meno, C., Pfister, V., Chen, L., Robertson, E., & Hamada, H. (2002). Nodal antagonists in the anterior visceral endoderm prevent the formation of multiple primitive streaks. *Developmental Cell*, *3*(5), 745–756.

Schier, A. F. (2003). Nodal signaling in vertebrate development. *Annual Review of Cell and Developmental Biology*, *19*(1), 589–621.

Schmierer, B., & Hill, C. S. (2007). TGFbeta-SMAD signal transduction: molecular specificity and functional flexibility. *Nature Reviews. Molecular Cell Biology*, *8*(12), 970—982. https://doi.org/10.1038/nrm2297

Stainier, D. Y. R. (2002). A glimpse into the molecular entrails of endoderm formation. *Genes & Development*, *16*(8), 893–907.

Tam, P. P., & Behringer, R. R. (1997). Mouse gastrulation: the formation of a mammalian body plan. *Mechanisms of Development*, *68*(1–2), 3–25.

Vallier, L., Touboul, T., Chng, Z., Brimpari, M., Hannan, N., Millan, E., Smithers, L. E., Trotter, M., Rugg-Gunn, P., & Weber, A. (2009). Early cell fate decisions of human embryonic stem cells and mouse epiblast stem cells are controlled by the same signalling pathways. *PloS One*, *4*(6), e6082.

Wu, G., Chen, Y.-G., Ozdamar, B., Gyuricza, C. A., Chong, P. A., Wrana, J. L., Massagué, J., & Shi, Y. (2000). Structural basis of Smad2 recognition by the Smad anchor for receptor activation. *Science*, *287*(5450), 92–97.

Yan, Y.-T., Liu, J.-J., Luo, Y., E, C., Haltiwanger, R. S., Abate-Shen, C., & Shen, M. M. (2002). Dual roles of Cripto as a ligand and coreceptor in the nodal signaling pathway. *Molecular and Cellular Biology*, *22*(13), 4439–4449.

Yeo, C.-Y., & Whitman, M. (2001). Nodal signals to Smads through Cripto-dependent and Cripto-independent mechanisms. *Molecular Cell*, *7*(5), 949–957.

Zeng, L., Fagotto, F., Zhang, T., Hsu, W., Vasicek, T. J., Iii, W. L. P., Lee, J. J., Tilghman, S. M., Gumbiner, B. M., & Costantini, F. (1997). The mouse Fused locus encodes Axin, an inhibitor of the Wnt signaling pathway that regulates embryonic axis formation. *Cell*, *90*(1), 181–192.

Zorn, A. M., & Wells, J. M. (2007). Molecular basis of vertebrate endoderm development. *International Review of Cytology*, *259*, 49–111.

Methods

Cell Culture

LSM3, PS04, PS03 and CAV2 were previously established by our lab (Kojima et al., 2014) . FS09 was established following previously described protocol (Osteil et al., 2015) from Foxa2-Venus::Sox17-mCherry ESC lines (Burtscher et al., 2013). All cell lines were generated from 129 mice.

Epiblast stem cells (EpiSCs) were maintained in medium comprising of Knockout-DMEM (Gibco, Cat. No. 10829-018) and 20% knock-out serum (Gibco, Cat. No. 10828-028), supplemented with 1% non-essential amino-acid supplement, 1% Glutamax (Gibco, Cat. No. 35050061) and 0.1uM 2-Mercaptoethanol (Sigma-Aldrich, Cat. No. M6250), 10ng/mL recombinant Human basic fibroblast growth factor (bFGF, R&D Systems, Cat. No. 233-FB 025/CF) and 20ng/mL recombinant human/mouse/rat Activin-A protein (carrier free) (R&D Systems, Cat. No. 338-AC-050/CF). Cells were passaged after reaching 70% confluency onto plates coated with 0.1% gelatin and previously seeded with irradiated mouse embryonic fibroblasts (MEFs) at a density of 16,000 cells/cm^2.

To passage EpiSCs, 2mg/mL Collagenase IV (R&D Systems, Cat. No. 338-AC-050/CF) was added to the culture and incubated for 10 minutes at 37°C. Dissociated colonies were collected following a brief centrifugation and dissociated into single cell suspension using TrypLE Select (Gibco, Cat. No. 12563-011) 2min at room temperature (RT). EpiSCs were seeded at a density of 17,000 cells/cm^2 in the aforementioned medium supplemented with 10uM Y-27632 ROCK inhibitor (TOCRIS, Cat. No. 1254) and maintained at 37^{o}C with 5% CO2. ROCK inhibitor was removed after 24h.

In vitro differentiation

2D differentiation: EpiSCs were seeded onto a MEF coated 6 well plate. After 24 hours, media was supplemented separately with Activin A, Nodal (carrier free) (R&D Systems, Cat. No. 1315-ND-025) and Recombinant Human BMP-4(Gibco, Cat. No. PHC9534) at three concentrations of 50ng/mL, 100ng/mL and 200ng/mL. Cells were incubated for 48 hours with growth factor replenished with a media change after 24 hours. The cultures were treated with collagenase IV to sample the differentiating EpiSCs from the underlying MEF for analysis.

3D differentiation: EpiSCs were passaged at 60% confluency and resuspended in EB medium: RPMI 1640 media (ThermoFisher Scientific, Cat. No. 21870-076) and Knock-Out Serum (20%) supplemented with 1% non-essential amino-acid supplement, 1% Glutamax and 0.1uM 2-Mercaptoethanol. Single cells were seeded at 2 x10^6 cells per well with 10uM Y-27632 ROCK inhibitor (TOCRIS, Cat. No. 1254) in a 24 well AggreWell plate (StemCell Technologies, Cat. No. 34415) and centrifuged at 1000RPM for 3 minutes. After 24 hours, aggregates were lifted from the Aggrewell plate by gentle pipetting. Unaggregated cells and debris were removed by passing the well contents through a 40μm cell strainer (StemCell Technologies, Cat. No. 27305). Aggregates retained in the filter were then transferred into a 60mm culture dishes containing 4mL of EB media supplemented with either 100ng/mL Activin A or 100ng/mL Recombinant Mouse Nodal Protein (carrier free) (R&D Systems, Cat. No. 1315-ND-025).

Imaging

Samples were imaged on an Olympus IX70 Inverted Microscope with a Lumenera Infinity 3-1 camera and Infinity Analyze software (Release 5). Cells were imaged on each day of their timeline immediately prior to media change and sample collection. FS09cells were exposed for 200ms with Olympus U-RFL-T mercury lamp. Image processing was performed using ImageJ (Fiji; imagej.nih.gov/ij). To artificially colour and stack images captured with fluorescence, the native ImageJ function Image/Color/Merge Channels was used.

Flow Cytometry

Embryoid bodies were dissociated into a single-cell suspension using TrypLE Select (Gibco, Cat. No. 12563-011), centrifuged at 1000RPM for 5 minutes and washed with Dulbecco's Phosphate Buffered Saline (Gibco, Cat. No. 14190-144). Samples were fixed in 4% paraformaldehyde at 37^{o}C for 30 mins. Samples were analysed using the BD LSRII flow cytometry. A 455nm laser with a 530/30 bandpass filter was used to detect Foxa2:Venus Green and a 561nm laser with a 610/20 bandpass filter was used to detect Sox17:mCherry fluorescence in the FS09 reporter cell line. The collected data was analysed using FlowJo Software (version 10.5.3, Oregon, USA).

Western Blot

Sample preparation

Cells were resuspended in 50mL of RIPA buffer consisting of 1% Ipegal CA-630, 0.5% sodium deoxycholate, 0.1% SDS, 1mM DTT, 1x Complete Protease Inhibitor Cocktail (Sigma Aldrich, Cat. No. 11836145001), 1x PhosSTOP EASYPack (Roche, Cat. No. 04906845001) Phosphatase Inhibitor, 1.5% Triton X-100 in Dulbecco's Phosphate Buffered Saline and incubated at 4^{o}C for 45 minutes. Samples were centrifuged for 10 mins at 13000RPM at 4^{o}C and the supernatant containing soluble proteins was collected. Samples were made to a concentration of 0.5mg/mL and 5x SDS loading dye (5% β-mercaptoethanol, 0.02% Bromophenol Blue, 30% Glycerol, 10% Sodium dodecyl sulfate, 250mM pH 6.8 TrisCl) was added to the samples. Samples were heat inactivated at 90^{o}C for 10 mins.

Protein separation and transfer

A Novex Nu-PAGE Pre-cast 4-12% gradient Bis-Tris 12-well gel (Life Technologies, Cat. No. NP0322BOX) was loaded in an XCell SureLock Novex Mini-gel electrophoresis chamber (Life Technologies, Cat. No. EI0001). 1x Running buffer was made from 20x stock (50 mM MES, 50 mM Tris-Base, 0.1% SDS, 1 mM EDTA) with MilliQ-Ultrapure Water and added to the electrophoresis chamber. 15uL of protein sample was run against 9mL Novex Sharp Pre-stained Protein Standard (Invitrogen, Cat. No. LC5800) for 60 mins at 200V. Gels were transferred to Whatman Optitran BA-S 83 0.2 µm Nitrocellulose membranes (Sigma-Aldrich, Cat. No. 10439380) Transfer was run in a Mini Trans-Blot Electrophoretic Cell (BioRad Cat. No.1703930) in 1x Towbin Transfer buffer made from a 5x stock (50mM Tris-base, 200mM glycine) with 10% methanol for 60 mins at 90V at 4°C. Membranes were washed in 1x PBST made from 10x PBS stock (PBS tablets, MP Biomedicals, Cat. No. 2810305) and 0.001% Tween20 (Sigma-Aldrich, Cat. No. 9005-64-5).

Membranes were blocked in blocking agent as applicable for antibody for 60 mins before the primary antibodies were applied (1:1000 dilution) overnight whilst rocking at 4°C; Phospho-Smad2 monoclonal antibody (Ser465/467) (Cell Signaling Technology Cat. No. 3108), Phospho-Smad1 (Ser463/465)/ Smad5 (Ser463/465)/ Smad9 (Ser465/467) monoclonal antibody (Cell Signaling Technoloy Cat. No.

13820), Cripto polyclonal antibody (Merck Cat. No. 05-665), Anti-Active β-Catenin (anti-ABC) monoclonal antibody (Merck Cat. No. 05-665), Vinculin monoclonal antibody (Sigma-Aldrich (Cat. No. MFCD00162905). The following day, membranes were washed with PBST and secondary antibodies were applied for 60 mins at RT. Membranes were revealed using SuperSignal West Pico PLUS Chemiluminescent Substrate (ThermoFisher, Cat. No. 34580) as per manufacturer's instructions. Membranes were imaged with Fujifilm LAS4000 Luminescence Imager.

Western Blot Analysis

ImageJ (Fiji imagej.nih.gov/ij) was used to analyse western blot band intensity. Rectangular selection tool was used to select an area containing both sample band and control band for western blot image. The function Analyse>Gels>Plot Lanes was used to generate histograms representing relative density of area content. Area under peaks, corresponding to band density, was selected with the wand tool, and the function Analyse>Gels>Label Peaks was used to calculate area under the curve. A normalised percentage was calculated as (selected peak area)/(total size of all selected peaks) to normalise for background variation. Correlation between pSMAD1/5/8 and pSMAD2 band intensity was determined using Pearson correlation and two-tail probability was used to calculate the significance of the correlation coefficient.

Microfluidic quantitative PCR

RNA extraction and preparation

Snap frozen cell pellets had total RNA extracted using ISOLATE II RNA mini kit (Bioline, Cat. No. BIO-52073) following manufacturer's instructions. RNA concentration was determined using Nanodrop ND-1000 Spectrophotometer (ThermoFisher Scientific). Sample RNA was diluted to a concentration of 200ng/uL. Fluidigm cDNA Preparation Master Mix (Fluidigm, Cat. No. 100-642-B1) was used for reverse transcription as per manufacturer's instructions then was reverse transcribed to cDNA using reagents from the RT2 Microfluidics qPCR Reagent System kit (Qiagen, 330431), as per the manufacturer's protocol.

cDNA preamplification

cDNA was pre-amplified using the RT2 PreAMP Pathway Primer Mix. For amplification of Cell Lineage marker genes in Figure S2, the following commercial sets were used: (Qiagen, PAMM-508Z and PAMM-081Y), TGFb (Qiagen, PAMM-235Z) and EMT target genes (Qiagen, PAMM-090Z) (Gene lists in Supplementary Table S2). Custom made oligos were used for analysis of the FS09 and PS04 line (Supplementary Table 1) seen in Figure 2B. Microfluidic qPCR was performed on the sets of pre-amplified cDNA using above primer sets. Primers were pooled, with a final concentration of 100uM. Primers were applied to prepared samples and Fluidigm PreAmp MasterMix (Fluidigm, Cat. No. 1005580) was added to samples. The following pre-amplification steps were performed: Hold; 95°C/2min, 10 cycles of 95°C/15 sec, 60°C/4 mins. Remaining primers were removed with Exonuclease 1 (20U/mL), in an Exo1 reaction buffer (ThermoFisher Scientific, Cat. No. EN0851).

Microfluidic qPCR

The prepared samples were analysed on the Biomark HD system (Fluidigm) for microfluidic quantitative qPCR. Pre-amplified sample were prepared as follows: 2.5 µL of 2× SsoFast EvaGreen Supermix with low ROX (Biorad, Cat No. 172-5211), 0.25 µL 25× DNA Binding Dye (Fluidigm, Cat. No. 100-7609) and 2.25 µL of diluted sample were prepared. Primers were prepared in the following mix:

2.5 µL 2× Assay Loading Reagent (Fluidigm, 100-7611), 1× DNA Suspension Buffer (TEKnova, Cat. No. T0221), 0.25 µL of combined forward and reverse primers. Samples and primers were combined and loaded into a 96.96 Dynamic Array IFC plate (Fluidigm, Cat. No. BMK-M-96.96) and run on the Biomark System. See supplemental data for primer sequences.

Data analysis

Each set of primers resulted in a different dataset that was first analysed independently. Raw data were extracted using the Fluidigm Real-Time PCRAnalysis Software and subsequent analysis was performed in R software. Ct values flagged as undetermined or greater than the threshold (Ct>24) were set to NA (missing values). Samples with a measurement for only one housekeeping gene or samples with measurements for <30 genes were excluded from further analysis. Genes where over 30 samples had a measurement of NA were also excluded from further analysis. Delta Ct (dCt) was calculated by subtracting the average expression of five housekeeping genes from the sample gene expression. Then, once dCt was generated, all the data were pooled together, and normalised to eliminate the batch effect across the primer sets and the various IFC plates. Samples were carried out across the experimental procedures to ensure efficient normalisation. Then, PCA and DEGs analysis were performed using R. The different sets of primers did not allow for merging the data as the commercial sequences are unknown therefore primer efficiency is not similar. Statistical analysis were performed using rstatix. Raw files and codes for the analysis are available on https://github.com/PierreOsteil/NodalVSActivinEpiSC

Figure legends

Figure 1. SMAD pathway response to Activin A and Nodal treatment. (A) FS09 EpiSCs treated with Activin A, Nodal or BMP4 for 48 hours at concentrations of 50ng/mL, 100ng/mL and 200ng/mL. Untreated EpiSCs (no factor supplementation) as the control. Western blot analysis used antibodies for pSMAD2 and pSMAD1/5/8. **(B)** Quantification of western blot results (average band intensity) normalized against vinculin control. Cell samples assessed for expression of **(C)** *Eomes* **(D)** *Brachyury* and **(E)** *Sox17* by qPCR analysis. Fold change in log scale. Significance level determined by student's t-test. **(F)** Relative band intensity between pSMAD2 and pSMAD1/5/8 (blot results in Figure 1B). r: Pearson correlation coefficient. Rep: replicate. AU: arbitrary unit. Significance level determined by one-way ANOVA. Significance level: *p<0.5. **p<0.01. ***p<0.001.

Figure 2. Differentiation trajectories of EpiSCs treated by Activin A and Nodal. (A) PCA analysis with variable correlation plot of microfluidic qPCR on 2 EpiSC lines (PS04 and FS09) collected at Day 0, 2 and 4 of directed EB differentiation cultured in Activin or Nodal (100ng/mL) supplemented media, using custom-made oligos set. **(B)** Genes contribution to principal component axis 1 and 2. The longer the vector the more a particular gene is contributing to the axes. **(C,D)** Heatmap and hierarchical clustering of differentially expressed genes at Day 4 of differentiation in EpiSC lines treated with Activin or Nodal.

Figure 3. Detection of definitive endoderm precursors in FS09 epiblast stem cells differentiated in Activin A and Nodal-supplemented media. (A) Fluorescence visualization of FoxA2:Venus/Sox17:mCherry expressing cells in EBs in Activin, Nodal or no-factor control in a 4-day timeline. Fluorescence image is overlaid on brightfield (BF) image. **(B)** Temporal profile of changes in the population of Foxa2:Venus-positive, Sox17-mCherry-positive and dual positive cells in the embryoid bodies quantified by flow cytometry. **(C)** Representative BF images and FoxA2:Venus/Sox17:mCherry fluorescent images of the three populations of reporter-expressing cells by flow cytometry at D2 of differentiation. Quantification of population fluorescence represented as contour map with 610nm excitation capturing mCherry and 530nm FoxA2. *EB: Embryoid bodies. BF: Brightfield.*

Figure 4. TGFβ/SMAD signalling activity in FS09 epiblast stem cells differentiated in Activin A and Nodal-supplemented media. Profiles of pSMAD expression over the 4 days of differentiation visualised by **(A)** western blot analysis and quantified by band intensity measurement in **(B).** pSMAD2 and pSMAD1/5/8 normalized against vinculin control. Asterisk colour denotes level of significance. **(C)** Temporal profile of expression of membrane anchored and soluble Cripto over 4 days of differentiation. Vinculin: reference control.

Figure 5. WNT signalling activity in FS09 epiblast stem cells differentiated in Activin A and Nodal-supplemented media. (A) Profile of active β-catenin expression in the 4 days of differentiation, visualised by western blot analysis. Vinculin, reference control. **(B)** Temporal profile of the expression of WNT signalling factors and WNT-responsive genes over 4 days of differentiation. Data normalised on Day 0 level of expression.

Supplementary Figures

Supplementary Table S1. Primer list and sequences for in-house Biomark plate (used to generate data in Figure 2).

Supplementary Table S2. Gene lists for amplification of Cell Lineage marker genes in Figure S2. Column header for the following commercial sets: Lineage markers (Qiagen, PAMM-508Z and PAMM-081Y), TGFb (Qiagen, PAMM-235Z) and EMT target genes (Qiagen, PAMM-090Z).

Supplementary Figure S1. Western blot images for; **(A)** EpiSCs treated with 50, 100 and 200 ng/mL. Antibody for **(i)** pSMAD2 or **(ii)** pSMAD1/5/8 is detected at ~60kDa. MagicMark XP Standard ladder was run with samples. **(B)** EpiSCs were treated for 4 days alongside a sample at Day 0 (D0). Antibody for **(i)** pSMAD2 or **(ii)** pSMAD1/5/8 is detected at ~60kDa. Novex Sharp pre-stained ladder was run against samples and marked with pencil on membrane. **(C)** Antibody for Cripto detects membrane anchored Cripto at 36kDa and soluble Cripto at 18kDa. Novex Sharp pre-stained ladder was run against samples and marked with pencil on membrane. **(D)** Antibody detects Active B-Catenin at ~110Da. Novex Sharp pre-stained ladder was run against samples and marked with pencil on membrane. **Abbreviations;** Activin A (A), Nodal (N), BMP4 (B), Control (C), Untreated (U).

Supplementary Figure S2. (A) PCA analysis with variable correlation plot of microfluidic qPCR on 4 EpiSC lines (PS04, PS03, CAV2 and LSM3) collected at Day 0, 2 and 4 of directed differentiation cultured in Activin or Nodal supplemented media, using the commercial set of oligos. **(B)** Genes contribution to principal component axis 1 and 2. The longer the vector the more a particular gene is contributing to the axes. **(C, D)** Heatmap and hierarchical clustering all genes for all days of differentiation in EpiSC lines treated with Activin or Nodal or untreated (Control).

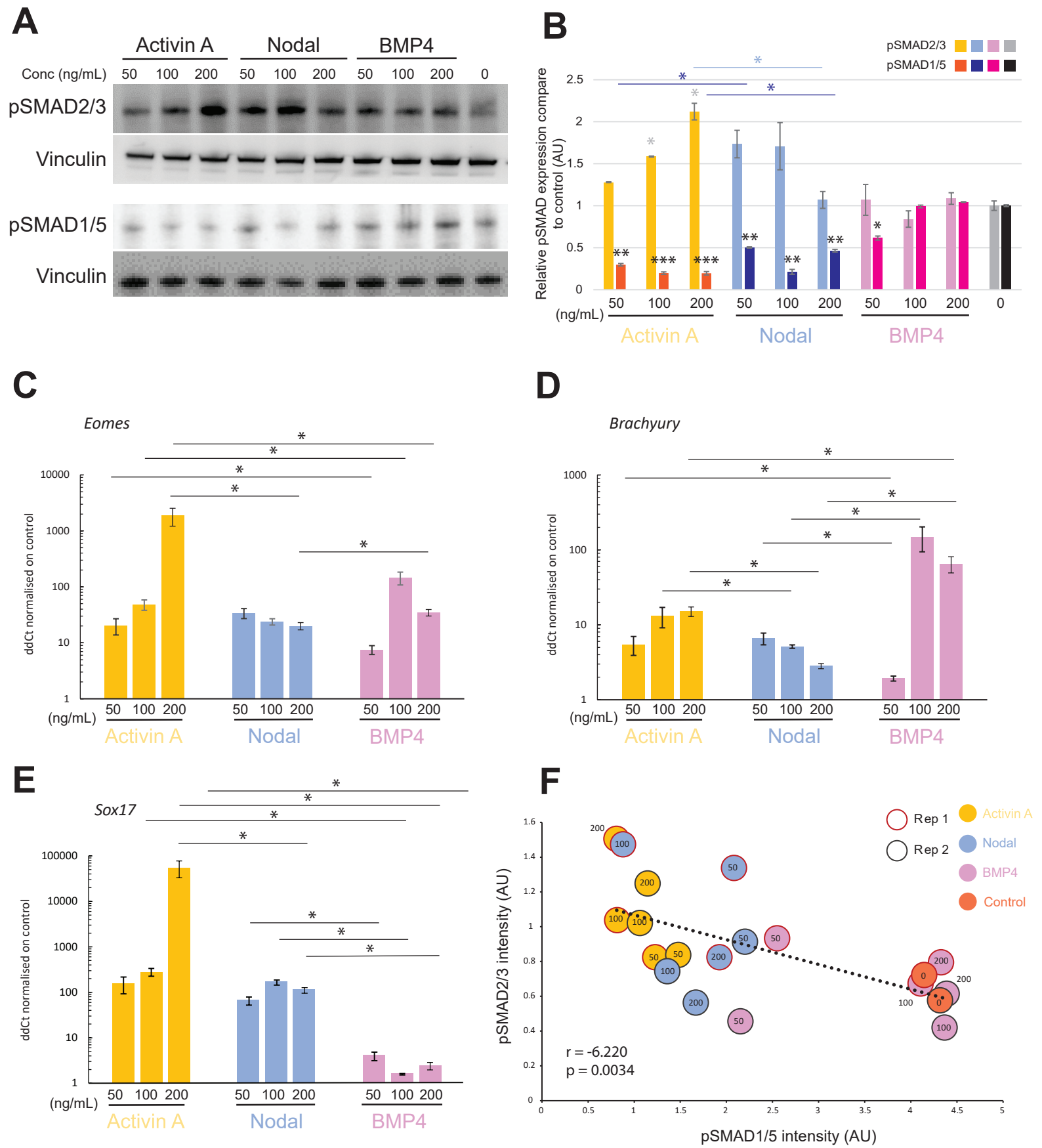
A
Activin A
Nodal
BMP4
Conc (ng/mL) 50 100 200 50 100 200 50 100 200 0
pSMAD2/3
Vinculin
pSMAD1/5
Vinculin
B
pSMAD2/3
pSMAD1/5
Relative pSMAD expression compare to control (AU)
(ng/mL)
Activin A
Nodal
BMP4
C
Eomes
ddCt normalised on control
(ng/mL)
Activin A
Nodal
BMP4
D
Brachyury
ddCt normalised on control
(ng/mL)
Activin A
Nodal
BMP4
E
Sox17
ddCt normalised on control
(ng/mL)
Activin A
Nodal
BMP4
F
Rep 1
Rep 2
Activin A
Nodal
BMP4
Control
pSMAD2/3 intensity (AU)
pSMAD1/5 intensity (AU)
r = -6.220
p = 0.0034

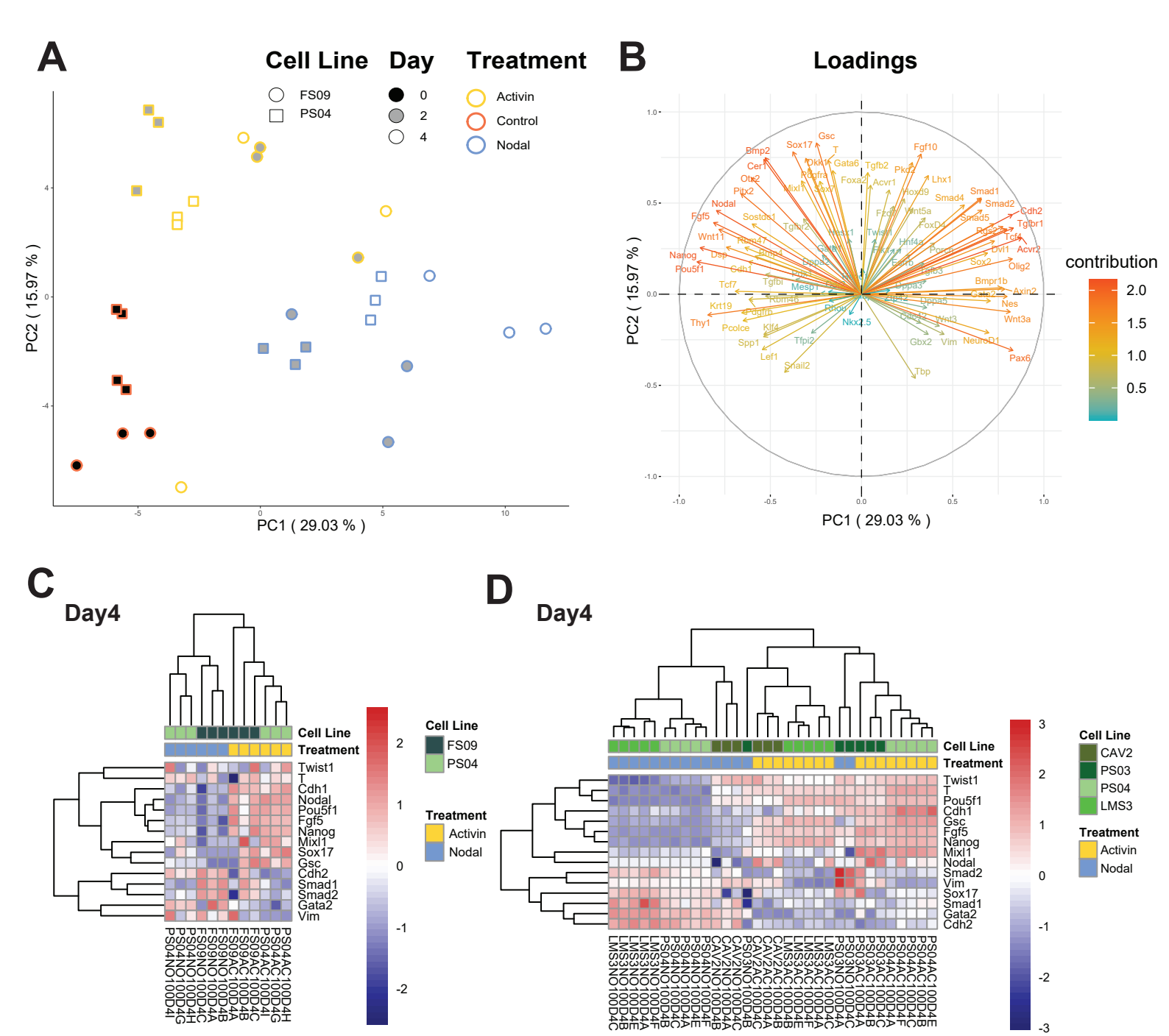
A
Cell Line
FS09
PS04
Day
0
2
4
Treatment
Activin
Control
Nodal
PC2 (15.97 %)
PC1 (29.03 %)
B
Loadings
PC2 (15.97 %)
PC1 (29.03 %)
contribution
2.0
1.5
1.0
0.5

C
Day4
Cell Line
Treatment
Twist1
T
Cdh1
Nodal
Pou5f1
Fgf5
Nanog
Mixl1
Sox17
Gsc
Cdh2
Smad1
Smad2
Gata2
Vim
Cell Line
FS09
PS04
Treatment
Activin
Nodal

D
Day4
Cell Line
Treatment
Twist1
T
Pou5f1
Cdh1
Gsc
Fgf5
Nanog
Mixl1
Nodal
Smad2
Vim
Sox17
Smad1
Gata2
Cdh2
Cell Line
CAV2
PS03
PS04
LMS3
Treatment
Activin
Nodal

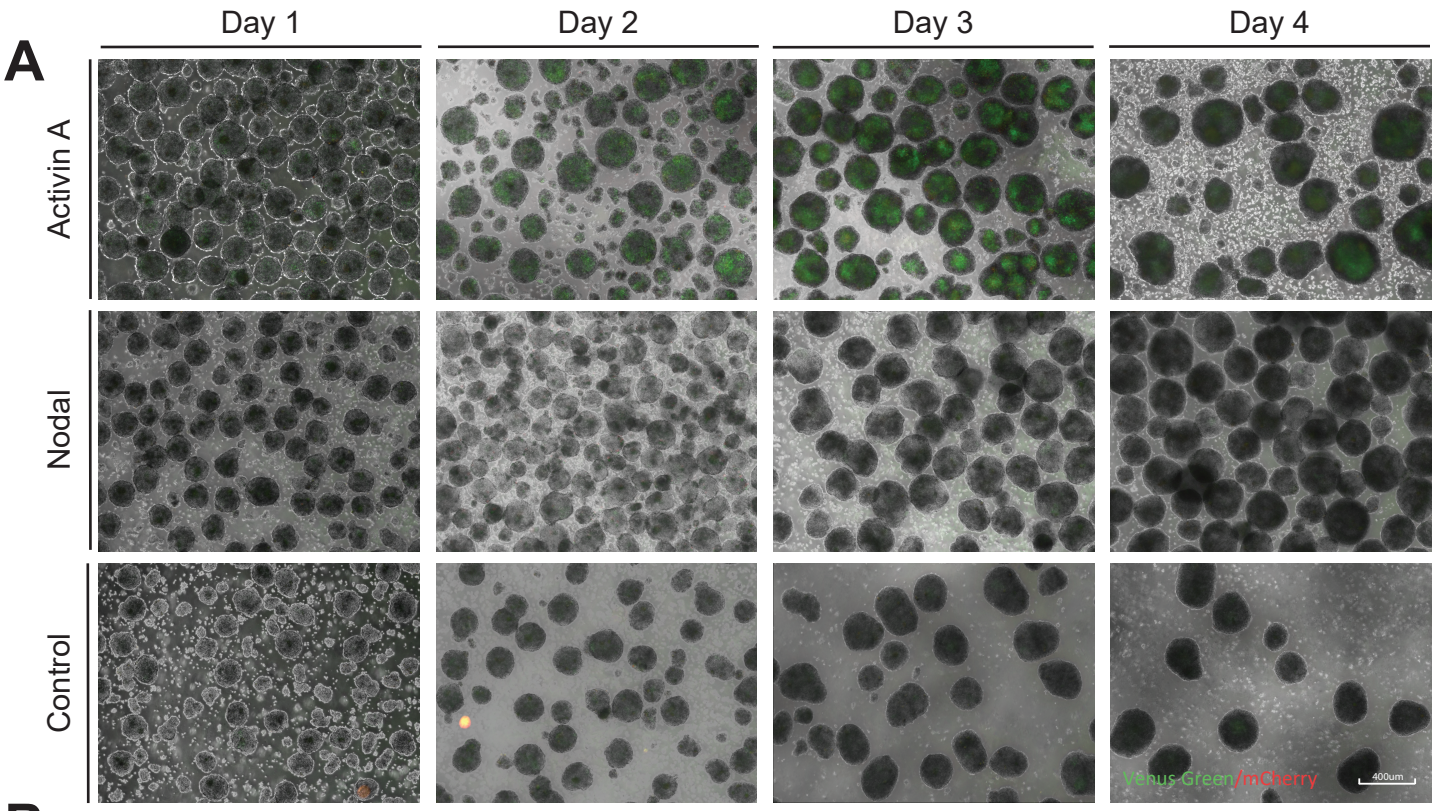
A
Day 1
Day 2
Day 3
Day 4
Activin A
Nodal
Control
Venus Green/mCherry
400um

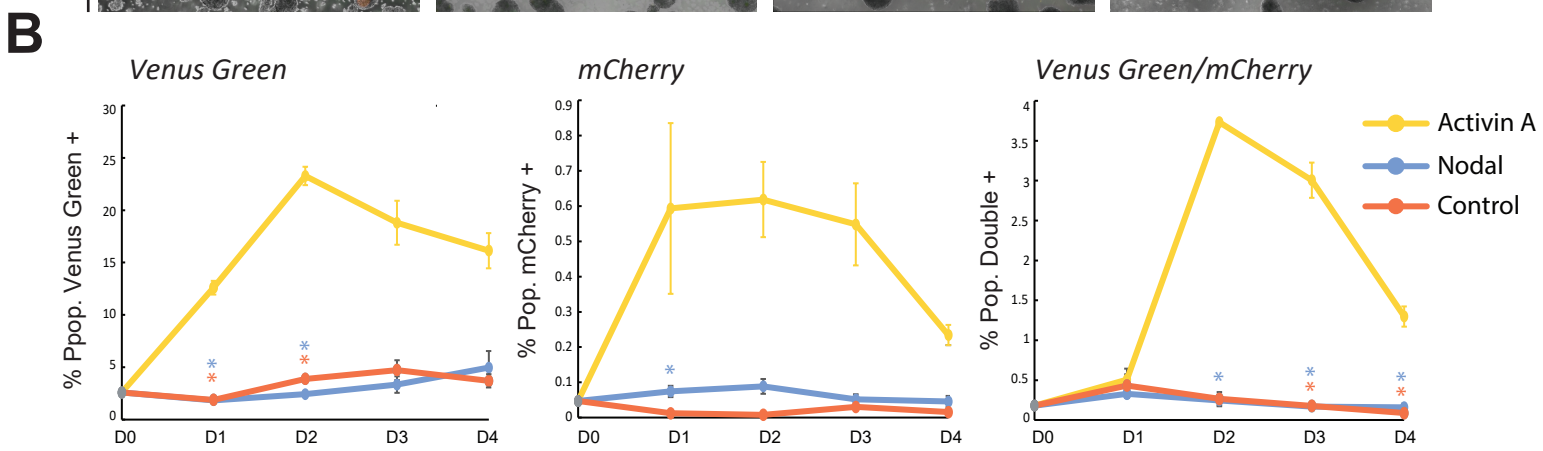
B
Venus Green
mCherry
Venus Green/mCherry
% Ppop. Venus Green +
% Pop. mCherry +
% Pop. Double +
D0
D1
D2
D3
D4
Activin A
Nodal
Control

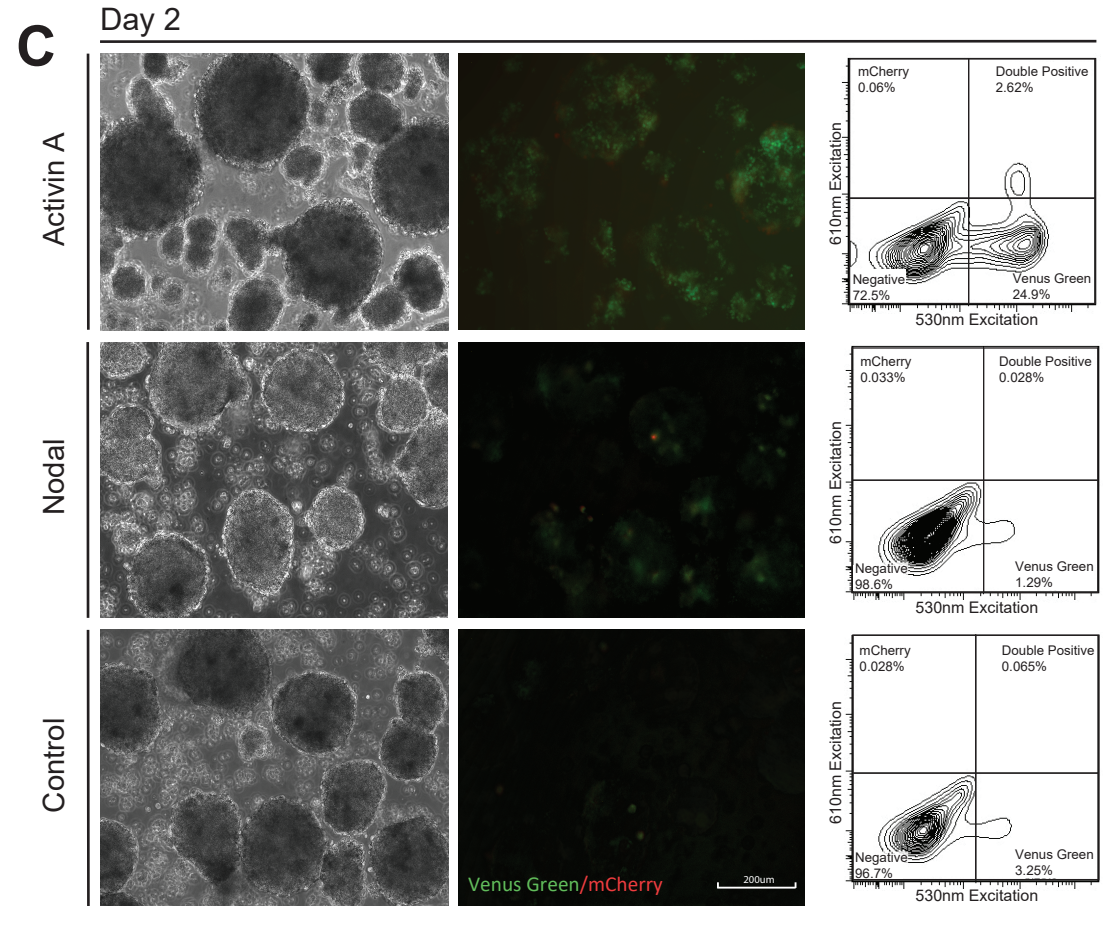
C
Day 2
Activin A
Nodal
Control
mCherry
0.06%
Double Positive
2.62%
Negative
72.5%
Venus Green
24.9%
mCherry
0.033%
Double Positive
0.028%
Negative
98.6%
Venus Green
1.29%
mCherry
0.028%
Double Positive
0.065%
Negative
96.7%
Venus Green
3.25%
610nm Excitation
530nm Excitation
Venus Green/mCherry
200um

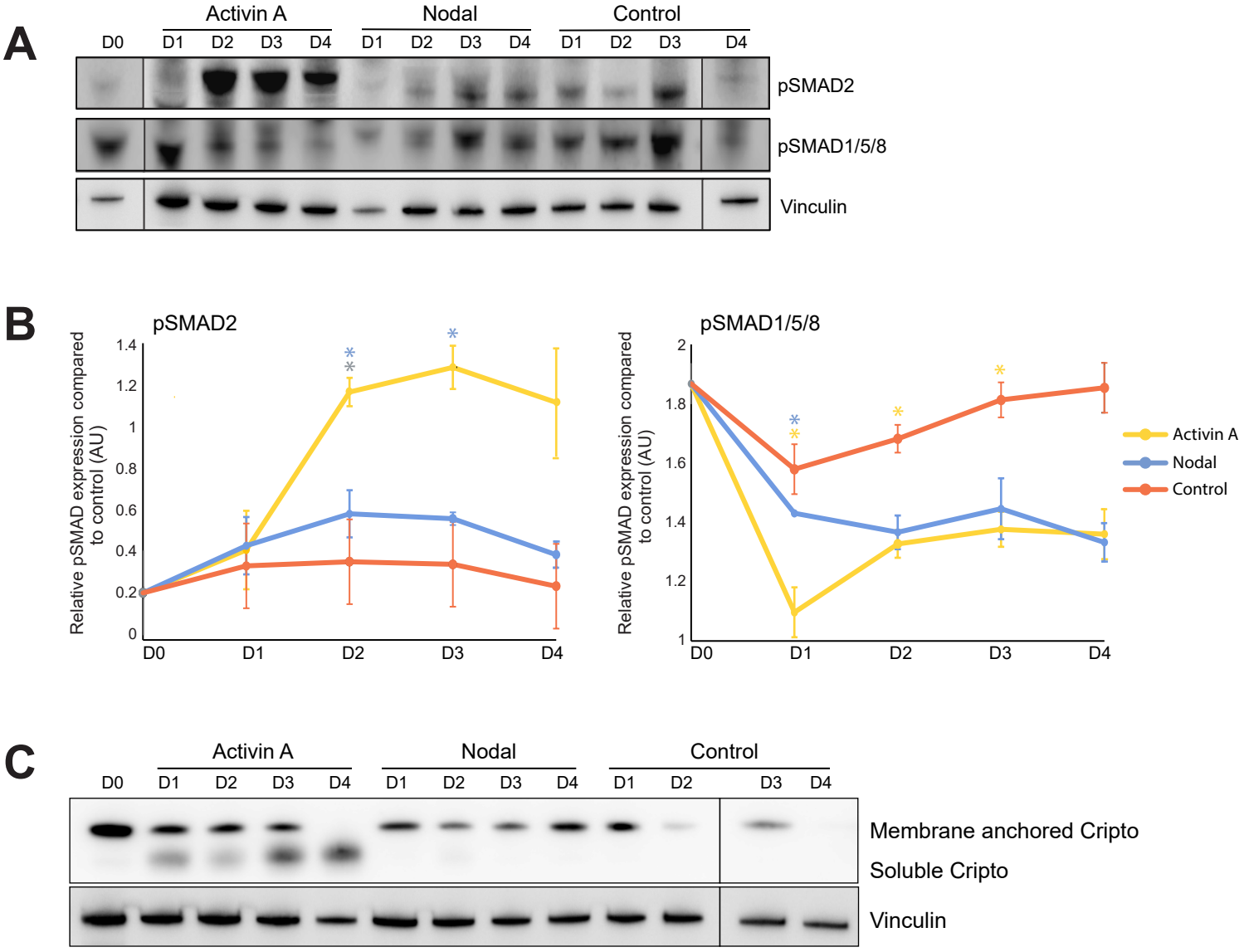
A
Activin A
Nodal
Control
D0
D1
D2
D3
D4
pSMAD2
pSMAD1/5/8
Vinculin
B
pSMAD2
pSMAD1/5/8
Relative pSMAD expression compared to control (AU)
Activin A
Nodal
Control
C
Membrane anchored Cripto
Soluble Cripto
Vinculin

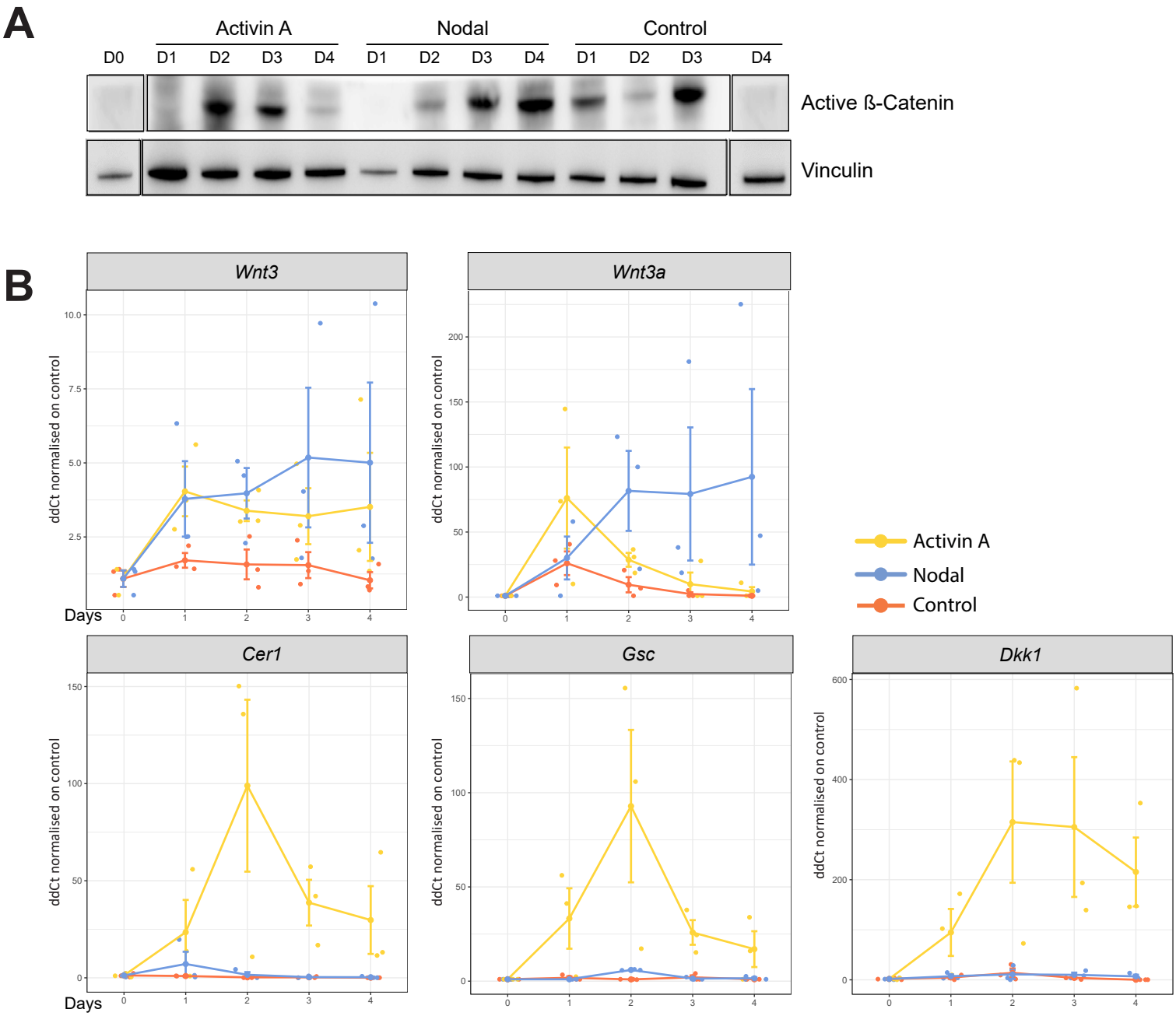
A
Activin A
Nodal
Control
D0
D1
D2
D3
D4
D1
D2
D3
D4
D1
D2
D3
D4
Active ß-Catenin
Vinculin
B
Wnt3
Wnt3a
Cer1
Gsc
Dkk1
ddCt normalised on control
Days
Activin A
Nodal
Control

A

i) pSMAD2

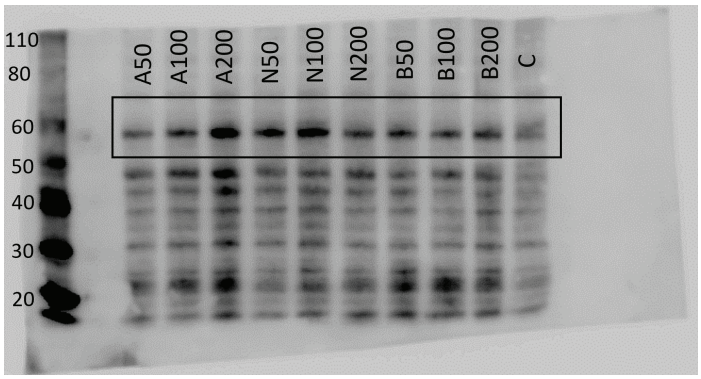

i) pSMAD1/5/8

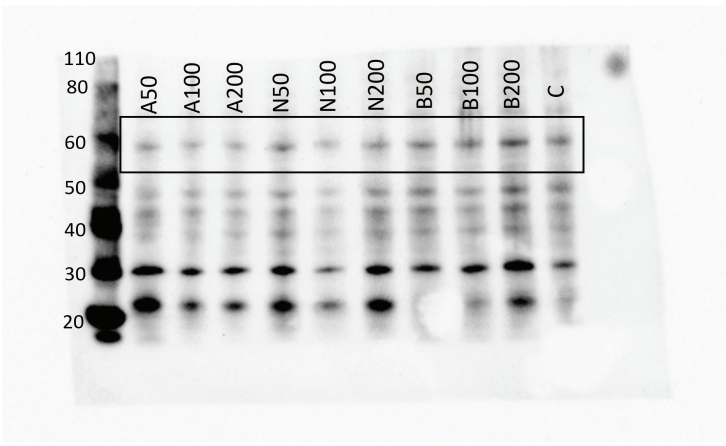

B

i) pSMAD2

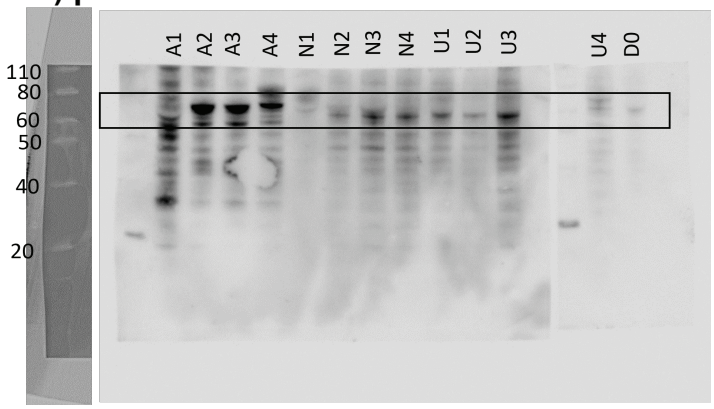

i) pSMAD1/5/8

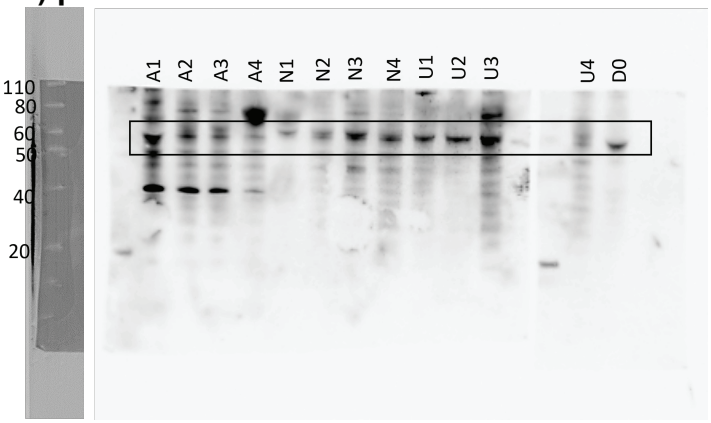

C

Cripto

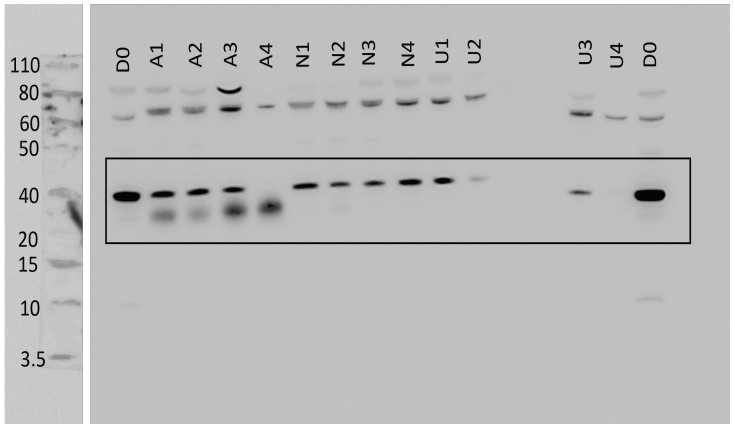

D

active β-catenin

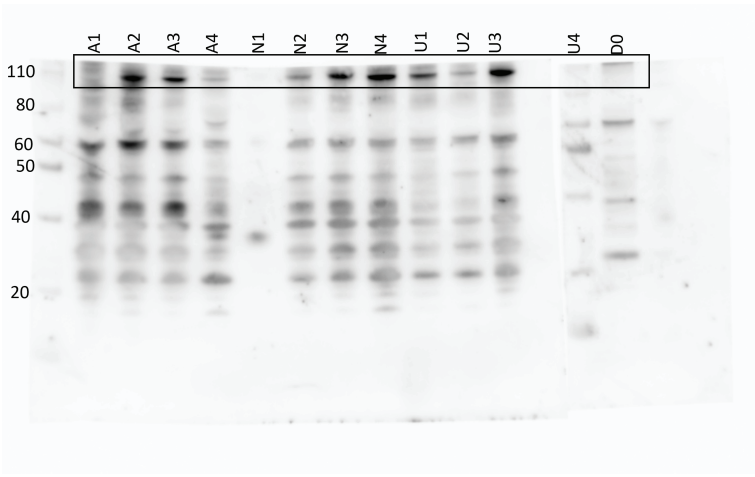

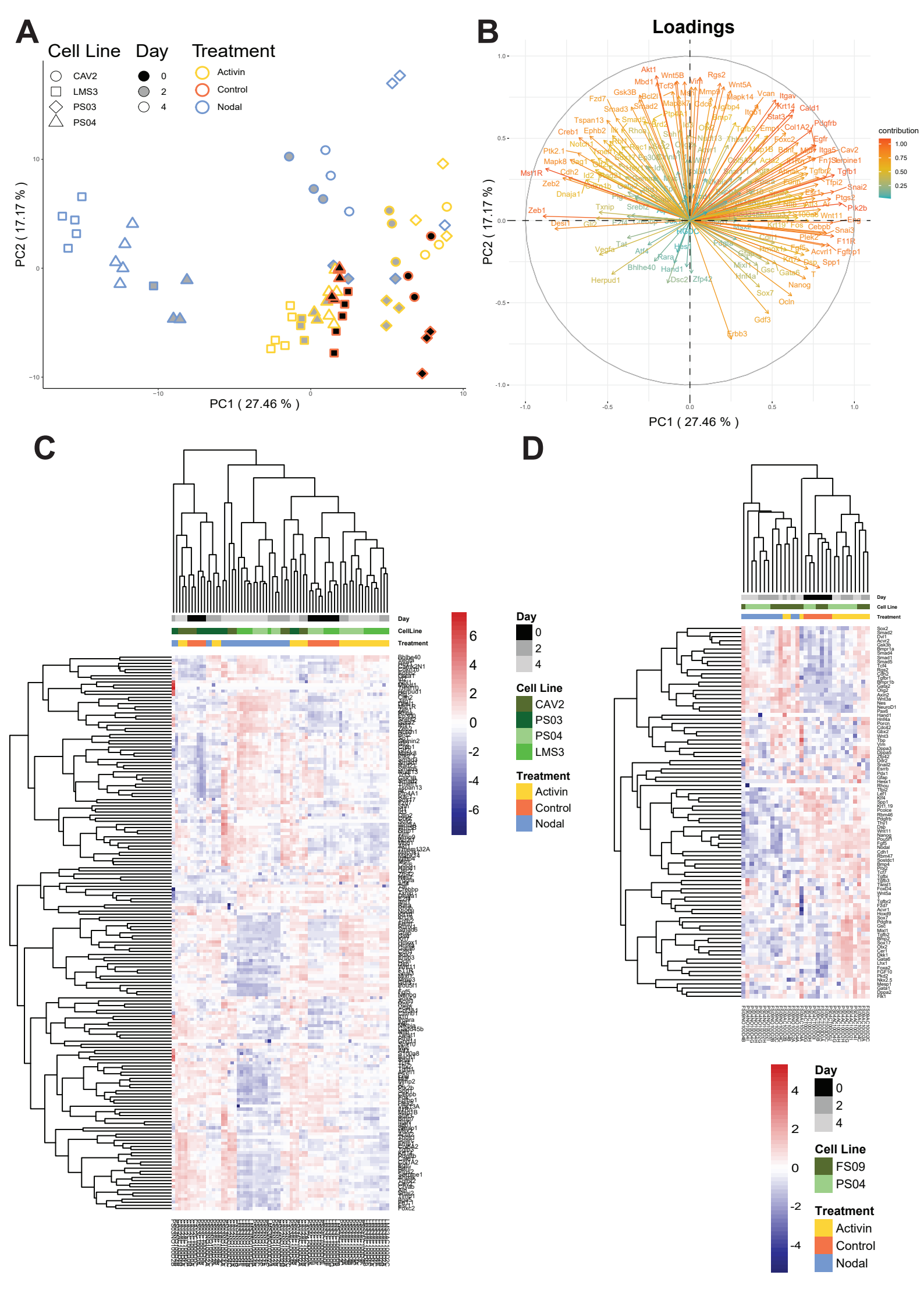
A
Cell Line
CAV2
LMS3
PS03
PS04
Day
0
2
4
Treatment
Activin
Control
Nodal
PC1 (27.46 %)
PC2 (17.17 %)
B
Loadings
contribution
1.00
0.75
0.50
0.25
PC1 (27.46 %)
PC2 (17.17 %)
C
Day
CellLine
Treatment
D
Day
Cell Line
Treatment
Day
0
2
4
Cell Line
CAV2
PS03
PS04
LMS3
Treatment
Activin
Control
Nodal
Day
0
2
4
Cell Line
FS09
PS04
Treatment
Activin
Control
Nodal